Modeling textures with total variation minimization and oscillating patterns in image processing

Luminita A. Vese* & Stanley J. Osher†

Department of Mathematics, University of California, Los Angeles

520 Portola Plaza, Los Angeles, CA 90095-1555, U.S.A.

E-mail addresses: lvese@math.ucla.edu, sjo@math.ucla.edu

UCLA C.A.M. Report 02-19, May 2002
To appear in Journal of Scientific Computing, Special Issue in the honor of Stanley Osher

Abstract

This paper is devoted to the modeling of real textured images by functional minimization and partial differential equations. Following the ideas of Yves Meyer in a total variation minimization framework of L. Rudin, S. Osher and E. Fatemi, we decompose a given (possible textured) image f into a sum of two functions $u+v$, where $u \in BV$ is a function of bounded variation (a cartoon or sketchy approximation of f), while v is a function representing the texture or noise. To model v we use the space of oscillating functions introduced by Yves Meyer, which is in some sense the dual of the BV space. The new algorithm is very simple, making use of differential equations and is easily solved in practice. Finally, we implement the method by finite differences, and we present various numerical results on real textured images, showing the obtained decomposition $u+v$, but we also show how the method can be used for texture discrimination and texture segmentation.

Keywords: functional minimization, partial differential equations, oscillating functions, functions of bounded variation, finite differences, texture modeling, image analysis.

1 Introduction

In many problems of image analysis, we have an observed image f, representing a real scene. The image f may contain noise (some random pattern of zero mean for instance) and/or texture (some repeated pattern of small scale details). The image processing task is to extract the most meaningful information from f. This is usually formulated as an inverse

*Supported in part by NSF ITR-0113439, ONR N00014-02-1-0015, and NIH P20MH65166.
†Supported in part by NSF DMS-0074735, ONR N00014-97-1-0027 and NIH P20MH65166.

problem: given f, find another image u, "close" to f, such that u is a cartoon or simplification of f. In general, u is an image formed by homogeneous regions and with sharp boundaries. Most models assume the following relation between f and u: $f = u + v$, where v is noise or small scale repeated detail (texture), and extract only the u component from f. Usually, the component v is not kept, assuming that this models the noise. In this category, we mention Rudin-Osher-Fatemi [22], Mumford-Shah [18], Perona-Malik [20], Alvarez-Guichard-Lions-Morel [2], Chambolle-Lions [10], Aubert-Vese [5], among many others. These models have the ability of computing optimal piecewise-smooth approximations u of u_0, while noise or small repeated patterns are removed from the image.

In some cases, the v component is important, especially if it represents texture. Texture can be defined as a repeated pattern of small scale details. The noise is also a pattern of small scale details, but of random, uncorrelated values. Both types of patterns (additive noise or texture) can be modeled by oscillatory functions taking both positive and negative values, and of zero mean [17].

Following the ideas of Yves Meyer [17], we show in this paper how we can extract from f both components u and v, in a simple total variation minimization framework of Rudin-Osher-Fatemi [22]. The obtained decomposition can then be useful for segmentation of textured images and texture discrimination, among other possible applications. The textured component v is completely represented using only two functions (g_1, g_2). This is much simpler and much more efficient than in other techniques for textures, which use a large number of channels to represent a textured image.

To summarize, we propose in this paper a simple model, which combines the edge preserving model of ROF, with the texture preserving model of Y. Meyer. The technique used is by energy minimization and partial differential equations. We illustrate the benefits of the new decomposition on various numerical results and applications to texture discrimination and texture segmentation.

We review next the main two ingredients of the proposed model: the total variation minimization of Rudin-Osher-Fatemi (ROF) [22] for image denoising and restoration (see also Rudin-Osher [21]), and the space of oscillating functions introduced by Yves Meyer [17] to model texture or noise.

Let $f : \mathbb{R}^2 \to \mathbb{R}$ be a given image (we assume that the image initially defined on a rectangle in $\mathbb{R}^2$, has been extended by reflection to the entire space). We assume that $f \in L^2(\mathbb{R}^2)$. In real applications, the observed image f is just a noisy version of a true image u, or (as we will see in this paper), it is a textured image, and u would be a simple sketchy approximation or a cartoon image of f. In the presence of additive noise, the relation between u and f can be expressed by the linear model, introducing another function v, and such that

$$f(x, y) = u(x, y) + v(x, y).$$

In the Rudin-Osher-Fatemi restoration model [22], v represents noise or small scale repeated details, while u is an image formed by homogeneous regions, and with sharp edges. Given f, both u and v are unknown (if v is noise, we may know some statistics of v, such that it is of zero mean and given variance). In [22], the problem of reconstructing u from f is posed as a minimization problem in the space of functions of bounded variation $BV(\mathbb{R}^2)$, this space allowing for edges or discontinuities along curves. Their model, very efficient for

denoising images while keeping sharp edges, is

$$\inf_{u\in L^2} F(u) = \int |\nabla u| + \lambda \int |f-u|^2 dxdy, \tag{1}$$

where $\lambda > 0$ is a tuning parameter. The second term in the energy is a fidelity term, while the first term is a regularizing term, to remove noise or small details, while keeping important features and sharp edges.

Existence and uniqueness results for the above minimization problem can be found in [1], [10], [25], [3] (see also [4]). This problem has minimizers in the space $BV(I\!R^2)$ of functions of bounded variation, which is defined by [11]: $u \in BV(I\!R^2)$ iff $u \in L^1(I\!R^2)$ and

$$\sup_{\vec{g}} \Big\{ \int u \mathrm{div}\vec{g} dxdy : \vec{g} \in C_c^1(I\!R^2; I\!R^2), |\vec{g}| \leq 1 \Big\} < \infty. \tag{2}$$

If we denote by $v = f - u$ or $f = u + v$, then the above minimization problem can be written as:

$$\inf_{u\in BV} \Big\{ F(u) = \int |\nabla u| + \lambda \|v\|^2_{L^2},\ f = u + v \Big\}. \tag{3}$$

Formally minimizing $F(u)$ yields the associated Euler-Lagrange equation

$$u = f + \frac{1}{2\lambda} \mathrm{div}\Big(\frac{\nabla u}{|\nabla u|}\Big)$$

(for a correct form of the equation $0 \in \partial F(u)$ satisfied by a minimizer $u \in BV$, we refer the reader to [25]).

In practice, to avoid division by zero, the curvature term $\mathrm{div}\Big(\frac{\nabla u}{|\nabla u|}\Big)$ is approximated by $\mathrm{div}\Big(\frac{\nabla u}{\sqrt{\epsilon^2+|\nabla u|^2}}\Big)$, and the BV solution is obtained as the limit of smoother minimizers, as $\epsilon \to 0$, as in [1], [25]. This convention will be always made in this paper.

Then, the function representing noise or texture in the ROF model is $v = f - u = -\frac{1}{2\lambda}\mathrm{div}\Big(\frac{\nabla u}{|\nabla u|}\Big)$, but this is not computed explicitly in the ROF model. Only the component u is kept in the ROF model.

Note that the above function v in the ROF model can be formally written as: $v = \mathrm{div}\vec{g}$, where $\vec{g} = (g_1, g_2)$ and $g_1 = -\frac{1}{2\lambda}\frac{u_x}{|\nabla u|}$, $g_2 = -\frac{1}{2\lambda}\frac{u_y}{|\nabla u|}$. We have that $g_1^2(x,y) + g_2^2(x,y) = \frac{1}{2\lambda}$ for all (x,y), so that $\|\sqrt{g_1^2+g_2^2}\|_{L^\infty} = \frac{1}{2\lambda}$ (later we will use the notation $|\vec{g}| = \sqrt{g_1^2+g_2^2}$).

In [17], Yves Meyer proves that the ROF model will remove the texture, if λ is small enough. In order to extract both the u component in BV and the v component as an oscillating function (texture or noise) from f, Yves Meyer [17] proposes the use of a space of functions, which is in some sense the dual of the BV space (see also condition (2)). On the topic of oscillations in non-linear analysis, we would also like to refer the reader to [19].

He introduces the following definition [17]:

Definition 1. *Let G denote the Banach space consisting of all generalized functions $v(x,y)$ which can be written as*

$$v(x,y) = \partial_x g_1(x,y) + \partial_y g_2(x,y),\ g_1, g_2 \in L^\infty(I\!R^2), \tag{4}$$

induced by the norm $\|v\|_*$ defined as the lower bound of all L^∞ norms of the functions $|\vec{g}|$ where $\vec{g} = (g_1, g_2)$, $|\vec{g}(x,y)| = \sqrt{g_1(x,y)^2 + g_2(x,y)^2}$ and where the infimum is computed over all decompositions (4) of v.

Y. Meyer also gives the following three results [17]:

Lemma 1. *If $v \in L^2(\mathbb{R}^2)$, then $|\int f(x,y)v(x,y)dxdy| \leq \|f\|_{BV}\|v\|_*$.*

Lemma 2. *If the norm of f in G does not exceed $\frac{1}{2\lambda}$, then the optimal Rudin-Osher-Fatemi decomposition of f is given by $u = 0$, $v = f$.*

Theorem 1. *Let f, u and v be three functions in $L^2(\mathbb{R}^2)$. If $\|f\|_* > \frac{1}{2\lambda}$, then the Rudin-Osher-Fatemi decomposition $f = u + v$ is characterized by the following two conditions:*

$$\|v\|_* = \frac{1}{2\lambda} \quad \textit{and} \quad \int u(x,y)v(x,y)dxdy = \frac{1}{2\lambda}\|u\|_{BV}.$$

In the above results, we have used the notation $\|u\|_{BV} := \int |\nabla u|$ for the total variation of u.

Y. Meyer shows that, if the v component represents texture or noise, then $v \in G$, and proposes the following new image restoration model:

$$\inf_u \Big\{ E(u) = \int |\nabla u| + \lambda \|v\|_*, \ f = u + v \Big\}. \tag{5}$$

As was justified by Y. Meyer, we shall see that the space G allows for oscillating functions v, and the oscillations are well measured by the norm $\|v\|_*$.

In the next section, we show how we can solve a variant of this model in practice, making use only of simple partial differential equations.

Other work for restoration of textured images by total variation minimization in a wavelet framework are by F. Malgouyres [15], [16]. Also, texture modeling by statistical methods was proposed by S.C. Zhu, Y.N. Wu and D. Mumford, in [27], [28], and by S. Casadei, S. Mitter and P. Perona in [7]. In the context of texture segmentation, we cite only a few related work, such as G. Koepfler, C. Lopez, J.-M. Morel [12], G. Sapiro [24], T.S. Lee, D. Mumford, A. Yuille [14], T.S. Lee [13], C. Ballester and M. Gonzalez [6], among many other. A recent work for segmentation of textured images using segmentation based active contour models in a Gabor transform framework, is proposed by B. Sandberg, T. Chan and L. Vese [23].

Finally, we would like to mention other work using $u + v$ models, but in different contexts. One was proposed by A. Chambolle and P.-L. Lions [10], where a given image f was decomposed into a sum $u + v$, such that $u \in BV(\Omega)$ and v was the smoother part of f, satisfying $\nabla v \in BV(\Omega)$. Another related work involving image decomposition was proposed by W.M. Wells, W.E.L. Grimson, R. Kikinis and F.A. Jolesz [26], in the context of adaptive segmentation and classification using statistical methods: the new data $Y = ln(X)$ (the logarithmic transformation of the initial data X), is decomposed into a sum of two other components, one being piecewise-constant (given by the mean intensities for each class) and the other one being an additive bias field, to represent intensity inhomogeneities.

2 Description of the model

We are motivated by the following approximation to the L^∞ norm of $|\vec{g}| = \sqrt{g_1^2 + g_2^2}$, for $g_1, g_2 \in L^\infty(I\!R^2)$:

$$\|\sqrt{g_1^2 + g_2^2}\|_{L^\infty} = \lim_{p\to\infty} \|\sqrt{g_1^2 + g_2^2}\|_{L^p}.$$

Then, we propose the following minimization problem, inspired by (5):

$$\inf_{u,g_1,g_2} \Big\{ G_p(u, g_1, g_2) = \int |\nabla u| + \lambda \int |f - u - \partial_x g_1 - \partial_y g_2|^2 dxdy + \mu \Big[\int \Big(\sqrt{g_1^2 + g_2^2} \Big)^p dxdy \Big]^{\frac{1}{p}} \Big\}, \tag{6}$$

where $\lambda, \mu > 0$ are tuning parameters, and $p \to \infty$.

The first term insures that $u \in BV(I\!R^2)$, the second term insures that $f \approx u + \mathrm{div}\vec{g}$, while the third term is a penalty on the norm in G of $v = \mathrm{div}\vec{g}$. Clearly, if $\lambda \to \infty$ and $p \to \infty$, this model is formally an approximation of the model (5) originally proposed by Y. Meyer.

Formally minimizing the above energy with respect to u, g_1, g_2, yields the following Euler-Lagrange equations:

$$u = f - \partial_x g_1 - \partial_y g_2 + \frac{1}{2\lambda} \mathrm{div}\Big(\frac{\nabla u}{|\nabla u|} \Big), \tag{7}$$

$$\mu \Big(\|\sqrt{g_1^2 + g_2^2}\|_p \Big)^{1-p} \Big(\sqrt{g_1^2 + g_2^2} \Big)^{p-2} g_1 = 2\lambda \Big[\frac{\partial}{\partial x}(u - f) + \partial^2_{xx} g_1 + \partial^2_{xy} g_2 \Big], \tag{8}$$

$$\mu \Big(\|\sqrt{g_1^2 + g_2^2}\|_p \Big)^{1-p} \Big(\sqrt{g_1^2 + g_2^2} \Big)^{p-2} g_2 = 2\lambda \Big[\frac{\partial}{\partial y}(u - f) + \partial^2_{xy} g_1 + \partial^2_{yy} g_2 \Big]. \tag{9}$$

In our numerical calculations, we have tested the model for different values of p, with $1 \le p \le 10$. The obtained results are very similar. The case $p = 1$ yields faster calculations per iteration, so we give here the form of the Euler-Lagrange equations in this case ($p = 1$):

$$u = f - \partial_x g_1 - \partial_y g_2 + \frac{1}{2\lambda} \mathrm{div}\Big(\frac{\nabla u}{|\nabla u|} \Big), \tag{10}$$

$$\mu \frac{g_1}{\sqrt{g_1^2 + g_2^2}} = 2\lambda \Big[\frac{\partial}{\partial x}(u - f) + \partial^2_{xx} g_1 + \partial^2_{xy} g_2 \Big], \tag{11}$$

$$\mu \frac{g_2}{\sqrt{g_1^2 + g_2^2}} = 2\lambda \Big[\frac{\partial}{\partial y}(u - f) + \partial^2_{xy} g_1 + \partial^2_{yy} g_2 \Big]. \tag{12}$$

If the domain is finite, with exterior normal to the boundary denoted by (n_x, n_y), the associated boundary conditions are:

$$\frac{\nabla u}{|\nabla u|}(n_x, n_y) = 0,$$
$$(f - u - \partial_x g_1 - \partial_y g_2) n_x = 0,$$
$$(f - u - \partial_x g_1 - \partial_y g_2) n_y = 0.$$

As we shall see in the section devoted to numerical results, the proposed minimization model (6) allows to extract from a given real textured image f the components u and v, such

that u is a sketchy (cartoon) approximation of f, and $v = div(g_1, g_2)$ represents the texture or the noise. In addition, the minimizer obtained for $\vec{g} = (g_1, g_2)$ allows us to discriminate two textures, by looking at the functions $|\vec{g}| = \sqrt{g_1^2 + g_2^2}$, $|g_1|$ or $|g_2|$.

2.1 Analytical remarks

We list here a few simple analytical remarks about the proposed models. We will use the following notation: for $u \in BV$, we denote its total variation by: $\|u\|_{BV} := \int |\nabla u|$. We assume that $f \in L^2$.

• In the standard Rudin-Osher-Fatemi model [22], the residual is given by:

$$f - u = -\frac{1}{2\lambda} K(u),$$

where $K(u)$ denotes the curvature operator, defined by $K(u) = \mathrm{div}\left(\frac{\nabla u}{|\nabla u|}\right)$.

• In the new model for $p \geq 1$, the residual is given by the same expression:

$$f - (u + v) = -\frac{1}{2\lambda} K(u).$$

• In the new model with $p = 1$, from equations (10)-(12), it is easy to show the following remarkable relation:

$$\mu = |\nabla K(u)|.$$

• In the new model with $p > 1$, from equations (7)-(9), we can easily show the following relations:

$$\mu \Big(\frac{\sqrt{g_1^2 + g_2^2}}{\|\sqrt{g_1^2 + g_2^2}\|_p} \Big)^{p-1} = |\nabla K(u)|,$$

$$\mu \|\sqrt{g_1^2 + g_2^2}\|_p = \int \sqrt{g_1^2 + g_2^2} \cdot |\nabla K(u)|.$$

If $\vec{g}$ is of constant magnitude, then the above relation involves the BV norm of $K(u)$, or the total variation of $K(u)$. If $\vec{g}$ is not of constant magnitude, then $\int |\vec{g}| \cdot |\nabla K(u)|$ can be viewed as a weighted BV norm of the curvature $K(u)$.

• **Lemma 3.** *If $\hat{u} = 0$, $\hat{\vec{g}} \in (L^p)^2$ is a minimizer of the problem (6), then $\|f - \mathrm{div}\hat{\vec{g}}\|_* \leq \frac{1}{2\lambda}$.*

Proof. We will have for any $u \in BV$ that:

$$\|u\|_{BV} + \lambda \|f - u - \mathrm{div}\hat{\vec{g}}\|_{L^2}^2 + \mu \||\vec{g}|\|_{L^p} \geq \lambda \|f - \mathrm{div}\hat{\vec{g}}\|_{L^2}^2 + \mu \||\hat{\vec{g}}|\|_{L^p},$$

or

$$\|u\|_{BV} + \lambda \|u\|_{L^2}^2 \geq 2\lambda \int u(f - \mathrm{div}\hat{\vec{g}}) dxdy.$$

Substituting in the above inequality u by ϵu, and taking $\epsilon \to 0$, we obtain:

$$\Big| \int u(f - \mathrm{div}\hat{\vec{g}}) dxdy \Big| \leq \frac{1}{2\lambda} \|u\|_{BV}.$$

The conclusion follows from this last inequality and from the duality between BV and $G \cap L^2$.

• **Lemma 4.** *If* $\hat{u} \in BV$, $\hat{\vec{g}} = (0,0)$ *is a minimizer of the problem (6), then* $\|\nabla(\hat{u} - f)\|_{L^q} \leq \frac{\mu}{2\lambda}$, *with* $\frac{1}{p} + \frac{1}{q} = 1$.

Proof. We will have for any $\vec{g} \in (L^p)^2$ that:

$$\|\hat{u}\|_{BV} + \lambda\|f - \hat{u} - \text{div}\vec{g}\|_{L^2}^2 + \mu\||\vec{g}|\|_{L^p} \geq \|\hat{u}\|_{BV} + \lambda\|f - \hat{u}\|_{L^2}^2,$$

or

$$\|\text{div}\vec{g}\|_{L^2}^2 + \mu\||\vec{g}|\|_{L^p} \geq 2\lambda \int (f - \hat{u})\text{div}\vec{g}dxdy = 2\lambda \int \nabla(\hat{u} - f) \cdot \vec{g}.$$

Substituting in the above inequality $\vec{g}$ by $\epsilon\vec{g}$, and taking $\epsilon \to 0$, we obtain:

$$|\int \nabla(\hat{u} - f) \cdot \vec{g}dxdy| \leq \frac{\mu}{2\lambda}\||\vec{g}|\|_{L^p}.$$

The conclusion follows from this last inequality and from the duality between L^p and L^q.

• **Lemma 5.** $u = 0$ and $\vec{g} = (0,0)$ is a minimizer of the problem (6) iff $\|f\|_* \leq \frac{1}{2\lambda}$ and $\|\nabla f\|_{L^q} \leq \frac{\mu}{2\lambda}$.

Proof. The direct implication is a consequence of the two previous results. The converse implication can be also verified by the previous techniques.

Remark. Lemma 3 could also be justified by applying Lemma 2 proved by Y. Meyer to $\hat{f} = f - \text{div}\hat{\vec{g}}$, for a fixed $\hat{\vec{g}}$.

Remark. Finally, we can apply Theorem 1 to our minimization problem (6) for a fixed $\vec{g}$. Then, this reduces to the classical Rudin-Osher-Fatemi minimization problem for a new data $f - \text{div}\vec{g}$, and we have the following property: for fixed $\vec{g}$, if $\|f - \text{div}\vec{g}\|_* > \frac{1}{2\lambda}$ and u is a minimizer, then $\|f - u - \text{div}\vec{g}\|_* = \frac{1}{2\lambda}$ and

$$\int u(x,y)f(x,y)dxdy - \int u^2(x,y)dxdy - \int u(x,y)\text{div}\vec{g}(x,y)dxdy = \frac{1}{2\lambda}\|u\|_{BV}.$$

Remark. We have verified some of these simple theoretical results by experimental calculations on simple images.

3 The numerical discretization of the model

To discretize the equations (7)-(9), we use a semi-implicit finite differences scheme and an iterative algorithm, based on a fixed point iteration. The equation in u is discretized following the schemes from [22] and [5]. Similar schemes are then used for the equations in g_1 and g_2. The initial guess that we use for the iterative algorithm is as follows: $u^0 = f$, $g_1^0 = -\frac{1}{2\lambda}\frac{f_x}{|\nabla f|}$, $g_2^0 = -\frac{1}{2\lambda}\frac{f_y}{|\nabla f|}$.

The details of our numerical algorithm are as follows. We use the classical notations $u_{i,j} \approx u(ih, jh)$, $f_{i,j} \approx f(ih, jh)$, $g_{1,i,j} \approx g_1(ih, jh)$ and $g_{2,i,j} \approx g_2(ih, jh)$, where $h > 0$ is the step space and (ih, jh) denotes a discrete point, for $0 \leq i, j \leq M$. To simplify the presentation, let us introduce the notation $H(g_1, g_2) = \left(\|\sqrt{g_1^2 + g_2^2}\|_p\right)^{1-p}\left(\sqrt{g_1^2 + g_2^2}\right)^{p-2}$.

The discrete forms of our equations are:

$$u_{i,j} = f_{i,j} - \frac{g_{1,i+1,j} - g_{1,i-1,j}}{2h} - \frac{g_{2,i,j+1} - g_{2,i,j-1}}{2h}$$
$$+\frac{1}{2\lambda h^2}\Big[\frac{u_{i+1,j} - u_{i,j}}{\sqrt{(\frac{u_{i+1,j}-u_{i,j}}{h})^2 + (\frac{u_{i,j+1}-u_{i,j-1}}{2h})^2}} - \frac{u_{i,j} - u_{i-1,j}}{\sqrt{(\frac{u_{i,j}-u_{i-1,j}}{h})^2 + (\frac{u_{i-1,j+1}-u_{i-1,j-1}}{2h})^2}}\Big]$$
$$+\frac{1}{2\lambda h^2}\Big[\frac{u_{i,j+1} - u_{i,j}}{\sqrt{(\frac{u_{i+1,j}-u_{i-1,j}}{2h})^2 + (\frac{u_{i,j+1}-u_{i,j}}{h})^2}} - \frac{u_{i,j} - u_{i,j-1}}{\sqrt{(\frac{u_{i+1,j-1}-u_{i-1,j-1}}{2h})^2 + (\frac{u_{i,j}-u_{i,j-1}}{h})^2}}\Big],$$

$$\mu H(g_{1,i,j}, g_{2,i,j})g_{1,i,j} = 2\lambda\Big[\frac{u_{i+1,j} - u_{i-1,j}}{2h} - \frac{f_{i+1,j} - f_{i-1,j}}{2h} + \frac{g_{1,i+1,j} - 2g_{1,i,j} + g_{1,i-1,j}}{h^2}$$
$$+\frac{1}{2h^2}(2g_{2,i,j} + g_{2,i-1,j-1} + g_{2,i+1,j+1} - g_{2,i,j-1} - g_{2,i-1,j} - g_{2,i+1,j} - g_{2,i,j+1})\Big],$$
$$\mu H(g_{1,i,j}, g_{2,i,j})g_{2,i,j} = 2\lambda\Big[\frac{u_{i,j+1} - u_{i,j-1}}{2h} - \frac{f_{i,j+1} - f_{i,j-1}}{2h} + \frac{g_{2,i,j+1} - 2g_{2,i,j} + g_{2,i,j-1}}{h^2}$$
$$+\frac{1}{2h^2}(2g_{1,i,j} + g_{1,i-1,j-1} + g_{1,i+1,j+1} - g_{1,i,j-1} - g_{1,i-1,j} - g_{1,i+1,j} - g_{1,i,j+1})\Big].$$

We introduce the following linearized equations:

$$u^{n+1}_{i,j} = f_{i,j} - \frac{g^n_{1,i+1,j} - g^n_{1,i-1,j}}{2h} - \frac{g^n_{2,i,j+1} - g^n_{2,i,j-1}}{2h}$$
$$+\frac{1}{2\lambda h^2}\Big[\frac{u^n_{i+1,j} - u^{n+1}_{i,j}}{\sqrt{(\frac{u^n_{i+1,j}-u^n_{i,j}}{h})^2 + (\frac{u^n_{i,j+1}-u^n_{i,j-1}}{2h})^2}} - \frac{u^{n+1}_{i,j} - u^n_{i-1,j}}{\sqrt{(\frac{u^n_{i,j}-u^n_{i-1,j}}{h})^2 + (\frac{u^n_{i-1,j+1}-u^n_{i-1,j-1}}{2h})^2}}\Big]$$
$$+\frac{1}{2\lambda h^2}\Big[\frac{u^n_{i,j+1} - u^{n+1}_{i,j}}{\sqrt{(\frac{u^n_{i+1,j}-u^n_{i-1,j}}{2h})^2 + (\frac{u^n_{i,j+1}-u^n_{i,j}}{h})^2}} - \frac{u^{n+1}_{i,j} - u^n_{i,j-1}}{\sqrt{(\frac{u^n_{i+1,j-1}-u^n_{i-1,j-1}}{2h})^2 + (\frac{u^n_{i,j}-u^n_{i,j-1}}{h})^2}}\Big],$$

$$\mu H(g^n_{1,i,j}, g^n_{2,i,j})g^{n+1}_{1,i,j} = 2\lambda\Big[\frac{u^n_{i+1,j} - u^n_{i-1,j}}{2h} - \frac{f_{i+1,j} - f_{i-1,j}}{2h} + \frac{g^n_{1,i+1,j} - 2g^{n+1}_{1,i,j} + g^n_{1,i-1,j}}{h^2}$$
$$+\frac{1}{2h^2}(2g^n_{2,i,j} + g^n_{2,i-1,j-1} + g^n_{2,i+1,j+1} - g^n_{2,i,j-1} - g^n_{2,i-1,j} - g^n_{2,i+1,j} - g^n_{2,i,j+1})\Big],$$
$$\mu H(g^n_{1,i,j}, g^n_{2,i,j})g^{n+1}_{2,i,j} = 2\lambda\Big[\frac{u^n_{i,j+1} - u^n_{i,j-1}}{2h} - \frac{f_{i,j+1} - f_{i,j-1}}{2h} + \frac{g^n_{2,i,j+1} - 2g^{n+1}_{2,i,j} + g^n_{2,i,j-1}}{h^2}$$
$$+\frac{1}{2h^2}(2g^n_{1,i,j} + g^n_{1,i-1,j-1} + g^n_{1,i+1,j+1} - g^n_{1,i,j-1} - g^n_{1,i-1,j} - g^n_{1,i+1,j} - g^n_{1,i,j+1})\Big].$$

Introducing the notations:

$$c_1 = \frac{1}{\sqrt{(\frac{u^n_{i+1,j}-u^n_{i,j}}{h})^2 + (\frac{u^n_{i,j+1}-u^n_{i,j-1}}{2h})^2}}, \quad c_2 = \frac{1}{\sqrt{(\frac{u^n_{i,j}-u^n_{i-1,j}}{h})^2 + (\frac{u^n_{i-1,j+1}-u^n_{i-1,j-1}}{2h})^2}},$$

$$c_3 = \frac{1}{\sqrt{(\frac{u^n_{i+1,j}-u^n_{i-1,j}}{2h})^2 + (\frac{u^n_{i,j+1}-u^n_{i,j}}{h})^2}}, \quad c_4 = \frac{1}{\sqrt{(\frac{u^n_{i+1,j-1}-u^n_{i-1,j-1}}{2h})^2 + (\frac{u^n_{i,j}-u^n_{i,j-1}}{h})^2}},$$

and solving in each equation for $u_{i,j}^{n+1}$, $g_{1,i,j}^{n+1}$ and for $g_{2,i,j}^{n+1}$ respectively, we obtain:

$$u_{i,j}^{n+1} = \Big(\frac{1}{1+\frac{1}{2\lambda h^2}(c_1+c_2+c_3+c_4)}\Big)\Big[f_{i,j} - \frac{g_{1,i+1,j}^n - g_{1,i-1,j}^n}{2h} - \frac{g_{2,i,j+1}^n - g_{2,i,j-1}^n}{2h} + \frac{1}{2\lambda h^2}(c_1 u_{i+1,j}^n + c_2 u_{i-1,j}^n + c_3 u_{i,j+1}^n + c_4 u_{i,j-1}^n)\Big],$$

$$g_{1,i,j}^{n+1} = \Big(\frac{2\lambda}{\mu H(g_{1,i,j}^n, g_{2,i,j}^n) + \frac{4\lambda}{h^2}}\Big)\Big[\frac{u_{i+1,j}^n - u_{i-1,j}^n}{2h} - \frac{f_{i+1,j} - f_{i-1,j}}{2h} + \frac{g_{1,i+1,j}^n + g_{1,i-1,j}^n}{h^2} + \frac{1}{2h^2}(2g_{2,i,j}^n + g_{2,i-1,j-1}^n + g_{2,i+1,j+1}^n - g_{2,i,j-1}^n - g_{2,i-1,j}^n - g_{2,i+1,j}^n - g_{2,i,j+1}^n)\Big],$$

$$g_{2,i,j}^{n+1} = \Big(\frac{2\lambda}{\mu H(g_{1,i,j}^n, g_{2,i,j}^n) + \frac{4\lambda}{h^2}}\Big)\Big[\frac{u_{i,j+1}^n - u_{i,j-1}^n}{2h} - \frac{f_{i,j+1} - f_{i,j-1}}{2h} + \frac{g_{2,i,j+1}^n + g_{2,i,j-1}^n}{h^2} + \frac{1}{2h^2}(2g_{1,i,j}^n + g_{1,i-1,j-1}^n + g_{1,i+1,j+1}^n - g_{1,i,j-1}^n - g_{1,i-1,j}^n - g_{1,i+1,j}^n - g_{1,i,j+1}^n)\Big].$$

As it can be noticed from the above formula, we have used the following approximation of the mixed derivatives:

$$\partial_{xy}^2 g_1(i,j) \approx \frac{1}{2h^2}(2g_{1,i,j} + g_{1,i-1,j-1} + g_{1,i+1,j+1} - g_{1,i,j-1} - g_{1,i-1,j} - g_{1,i+1,j} - g_{1,i,j+1}),$$

and similarly for g_2. We have also tested another approximation to the mixed derivatives, which is:

$$\partial_{xy}^2 g_1(i,j) \approx \frac{1}{4h^2}(g_{1,i+1,j+1} + g_{1,i-1,j-1} - g_{1,i+1,j-1} - g_{1,i-1,j+1}),$$

which also gave good results.

In practice, we set $h = 1$ and in our computer algorithm, we employ another fixed-point method: instead of $u_{i,j}^n$, $g_{1,i,j}^n$ and $g_{2,i,j}^n$, we always use the most recent value computed for each function at that point. At the boundary, we extend $u_{i,j}$ by reflection outside the domain, and a simple boundary condition for $\vec{g}$ would be Dirichlet boundary condition, which appears to work well in practice. We perform about 100 iterations for each experimental result. Other implicit or explicit schemes could have been constructed and used.

4 Numerical results

In this section, we show various numerical results using the proposed model. In all results, we take the space step $h = 1$, and we perform 100 iterations in most cases. Since in practice we have not noticed differences between the cases $p = 1$ and $p > 1$, we show the numerical results obtained with $p = 1$.

In Fig. 1 we consider a real textured image without noise for the initial data f. In Fig. 2 left we show the result u obtained with the ROF model, and in Fig. 2 right we show the residual $f - u$ (plus a constant for illustration purposes). We see that texture (in form of geometry) is still present in the residual $f - u$.

Next, in Fig. 3 we show the results obtained with the new model, for the same parameter λ. Note from Fig. 3 that $u + v$ represents very well the initial textured image f, and that

in the residual $f - u - v$ there is much less geometry and texture than by the ROF model. As expected, the image u in Fig. 3 is a sketchy approximation of f, while v is an oscillatory function (again, we have added a constant to the result v, for illustration purposes).

Similar results and comparisons are presented in Figures 4-5-6, for another textured image without noise, representing a fingerprint.

Then, we show comparisons and numerical results for both models with a noisy fingerprint image, shown in Fig. 7. The result u obtained with the ROF model is presented in Fig. 8 left, and the residual in Fig. 8 right. We see that the noise has been removed, but most of the texture is also removed from u.

In Fig. 9 we show results obtained with the new model applied to the noisy fingerprint image, for various parameters μ, but the same parameter λ. Note that, as expected, the proposed model keeps together the texture and the noise for smaller μ. It was also proved by Yves Meyer [17] that random additive noise of zero mean belongs to the same space G. So, the noise is considered as texture by the proposed model. Note that, for decreasing μ, more texture appears in the v component by the new model, but also more noise is kept.

In the next two examples (the fabric image and the wood image), we show that the new model can be used as a texture discriminator, by looking at the functions $|g_1|, |g_2|$ or $|\vec{g}| = \sqrt{g_1^2 + g_2^2}$. Even if the two textures are very similar, in these three components, their differences are clearly seen and can be discriminated.

Also, note that in general, texture discrimination is very expensive, since the image f is substituted by a sequence of images, transforms of f at different scale, orientation and phase parameters (such as Gabor transforms), yielding a large set of initial data. Here, just one component suffices to discriminate textures, like $|g_1|$, $|g_2|$, or $|\vec{g}|$. In general, if we do not know which component(s) should be used, then at most three channels are needed for texture discrimination and texture segmentation, in a multi-channel segmentation fashion.

Note that we do not need to perform a learning process of the texture and its statistics, as it is often done. Other methods for texture segmentation are using the so called "textons", as local averages of curvature of level lines and of the orientation of tangents to level lines (see for instance Koepfler-Lopez-Morel [12] and Chan-Vese [9]).

We show in Fig. 10 an initial image (fabric texture), and the results $u + v$, u and v obtained by the new model. In Fig. 11 we show the functions $|g_1|$, $|g_2|$, and $|\vec{g}|$. Here, we also show the contour between the two textures, extracted by applying the active contour model without gradient based segmentation from [8] [9] to the image $|g_1|$.

Similar results are shown in Figures 12-13, for another image (wood texture). Again, two of the functions $|g_1|$, $|g_2|$, and $|\vec{g}|$ help to discriminate the textures.

Finally, we show one more numerical result in Figures 14-15. We show the initial image f (a noisy version of a real image), the result $u + v$ and the u and v components. Note that $u + v$ is practically identical with f. The noise is kept in the v component and therefore in the sum $u + v$, but it has been removed from the u component.

Remark. Note that, since the residual $|f - u - v|$ is very small but not exactly zero, the proposed model produces in fact a decomposition of the form: $f = u + v + r$, where $r = -\frac{1}{2\lambda}\mathrm{div}\left(\frac{\nabla u}{|\nabla u|}\right)$. In the limit, as $\lambda \to \infty$, the model approximates a decomposition of the form $f = u + v$.

Figure 1: An initial textured image.

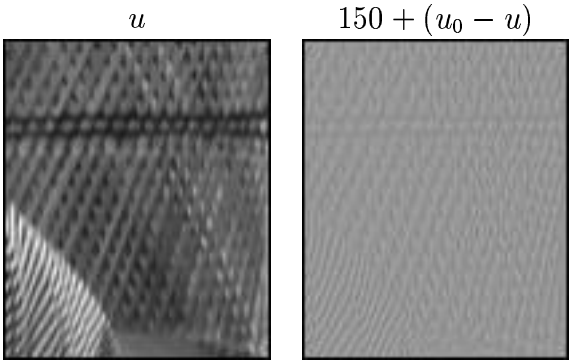

Figure 2: Result using the ROF model with $\lambda = 0.1$.

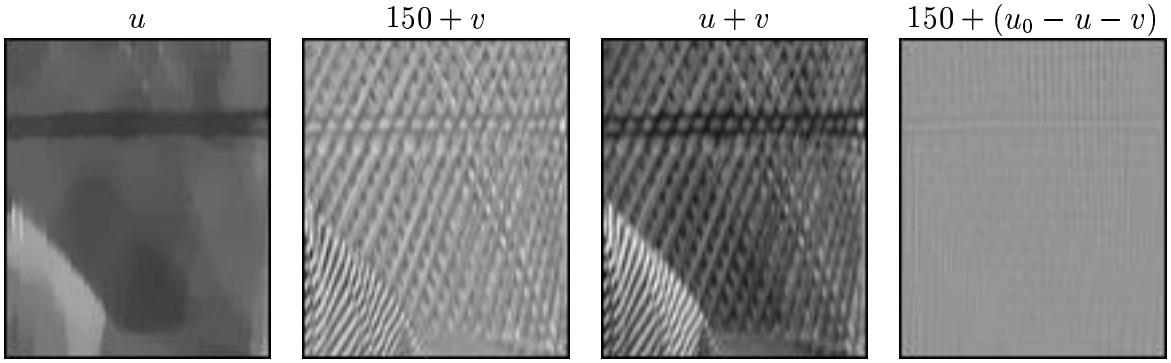

Figure 3: Result using the new model with $\lambda = 0.1$, $\mu = 0.1$.

Figure 4: An initial fingerprint image.

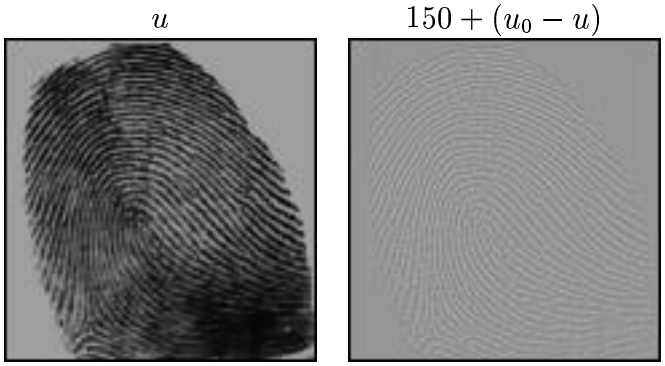

Figure 5: Result using the ROF model with $\lambda = 0.1$.

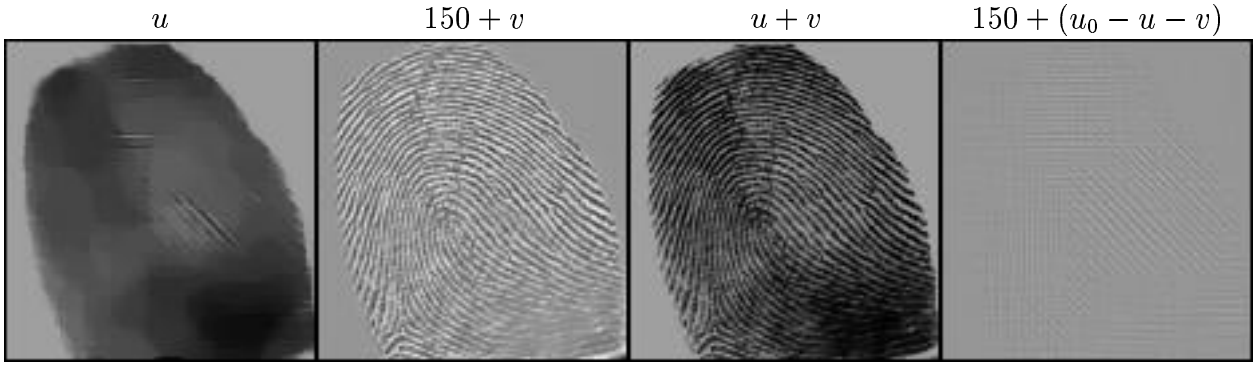

Figure 6: Result using the new model with $\lambda = 0.1$, $\mu = 0.1$.

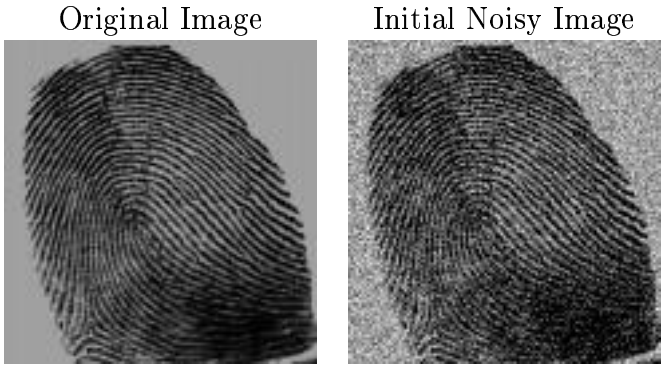

Figure 7: Original fingerprint image (left) and a noisy version u_0 (right).

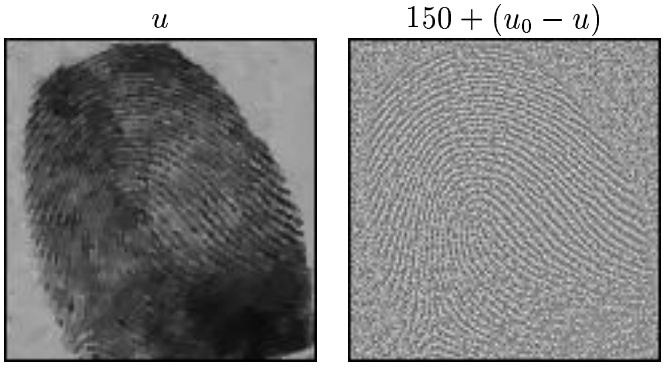

Figure 8: Result using the ROF model with $\lambda = 0.03$.

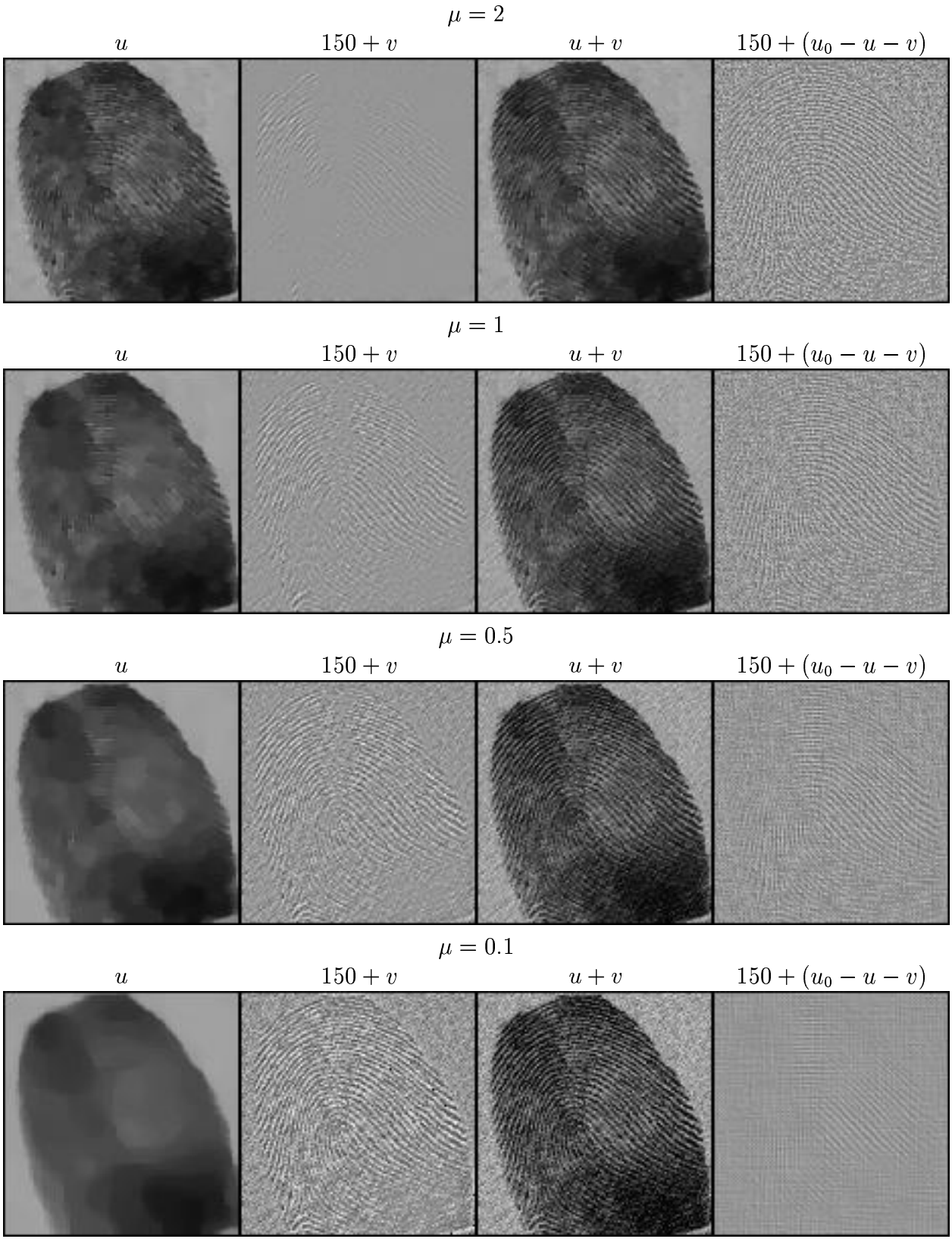

Figure 9: Results using the new model with $\lambda = 0.03$ and $\mu = 2;\ 1;\ 0.5;\ 0.1$.

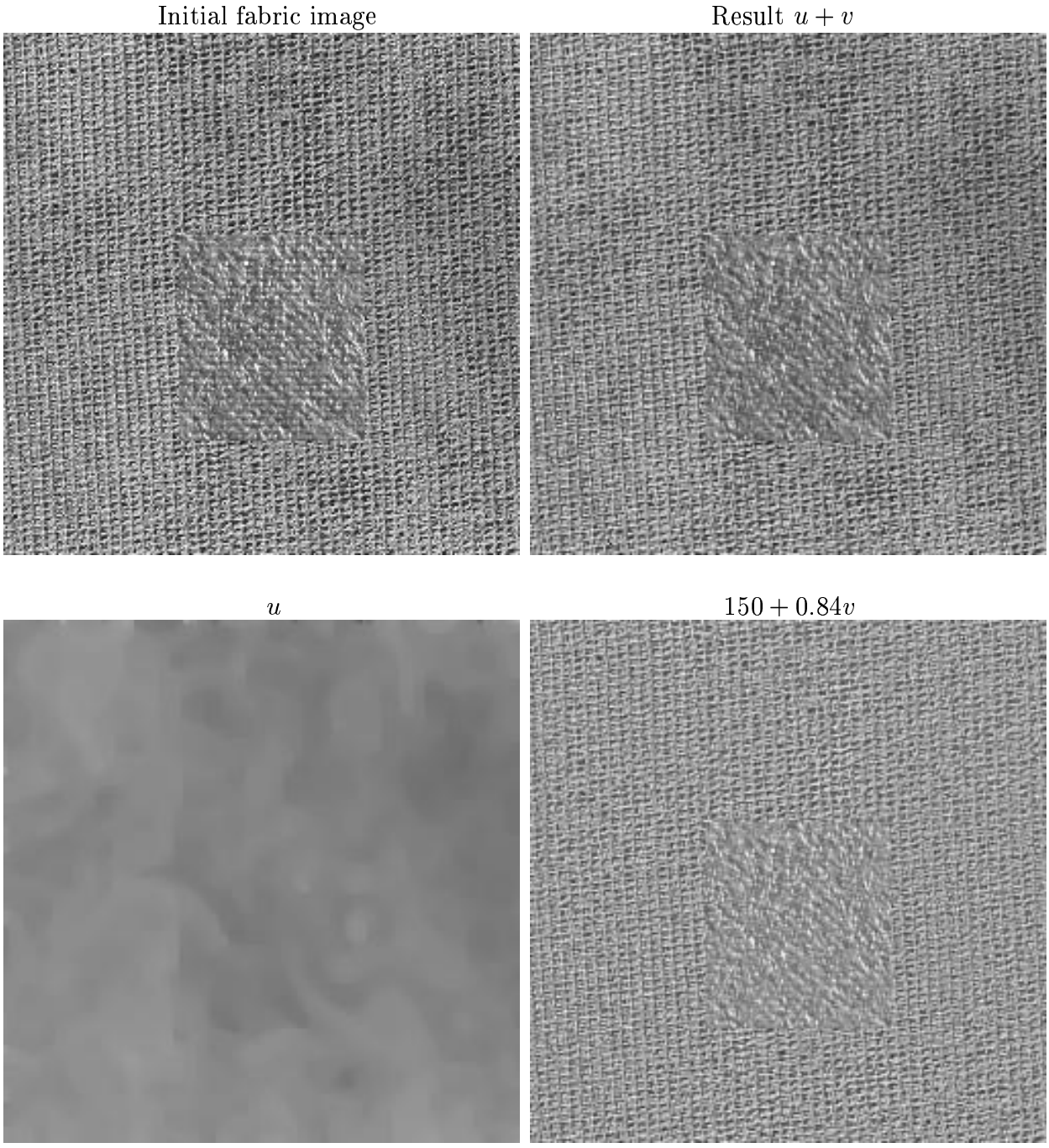

Figure 10: Results on the fabric image with the new model, with $\lambda = 0.01$ and $\mu = 0.001$.

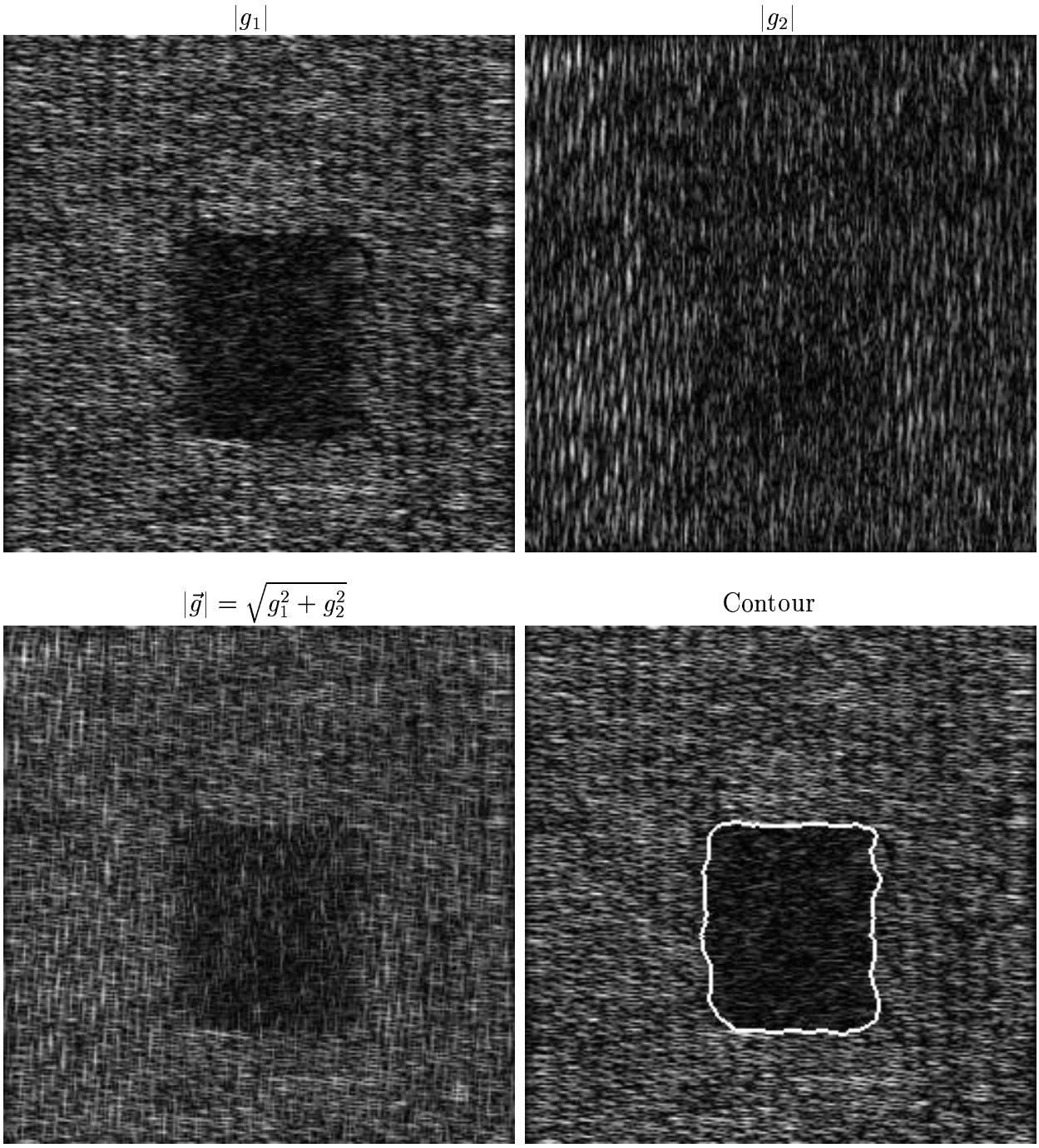

Figure 11: Results corresponding to the fabric image. Texture discrimination using the functions $|g_1|$, $|g_2|$, or $|\vec{g}|$. The detected contour is obtained by applying the active contour model without edges from [8], [9] to $|g_1|$.

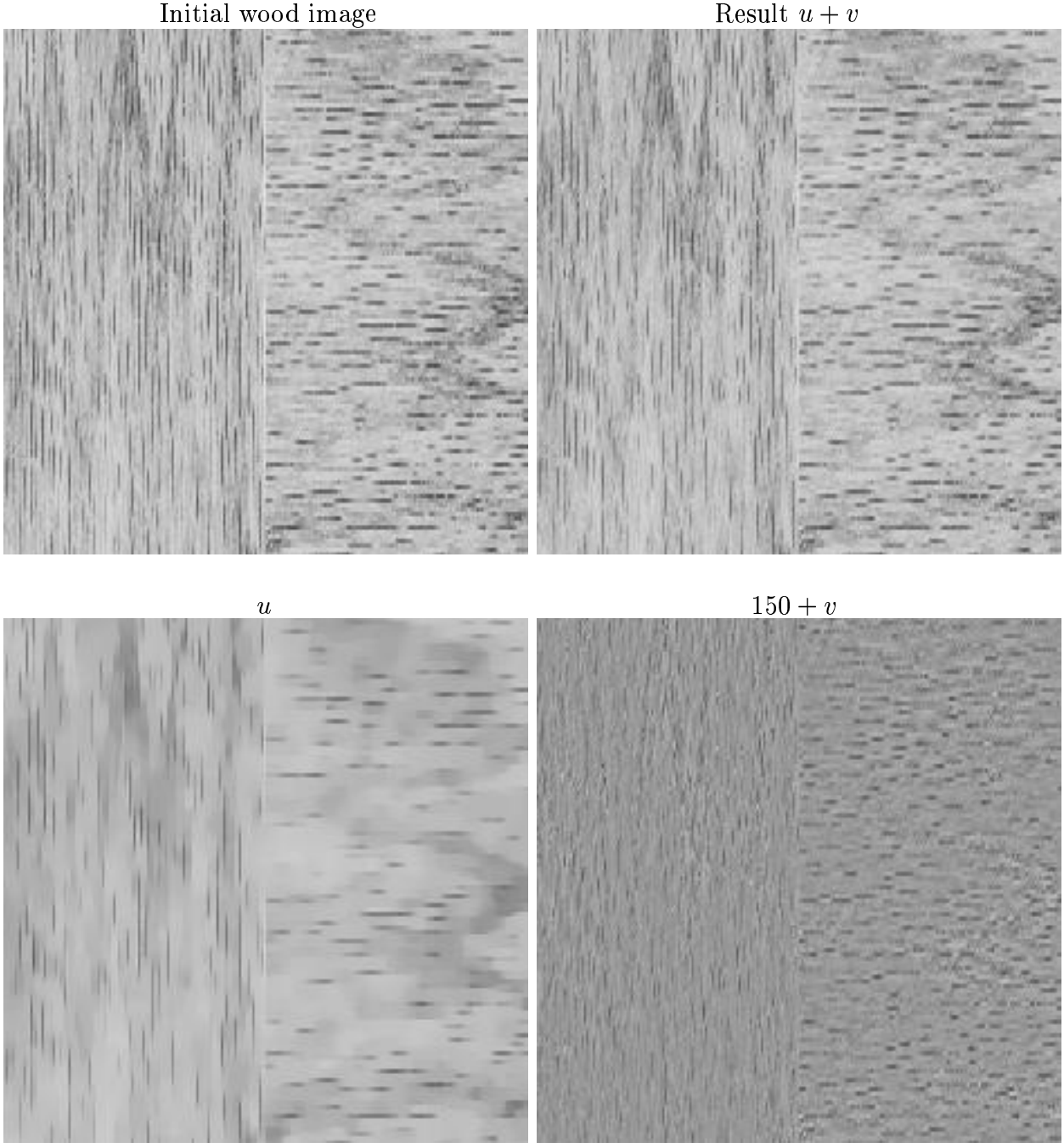

Figure 12: Results on the wood image with the new model, with $\lambda = 0.1$ and $\mu = 0.00001$.

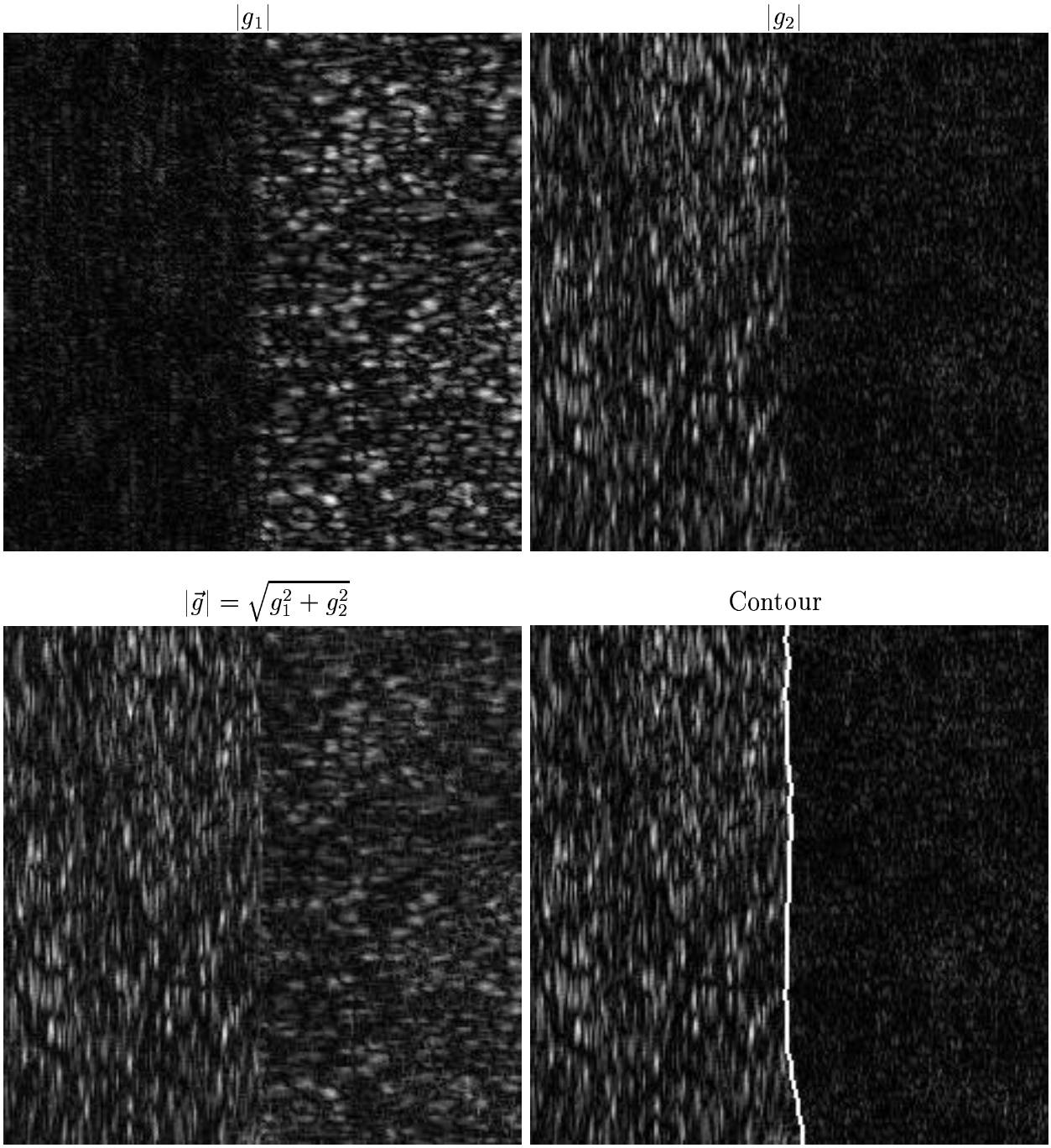

Figure 13: Results corresponding to the wood image. Texture discrimination using the functions $|g_1|$, $|g_2|$, or $|\vec{g}|$. The detected contour is obtained by applying the active contour model without edges from [8], [9] to $|g_2|$.

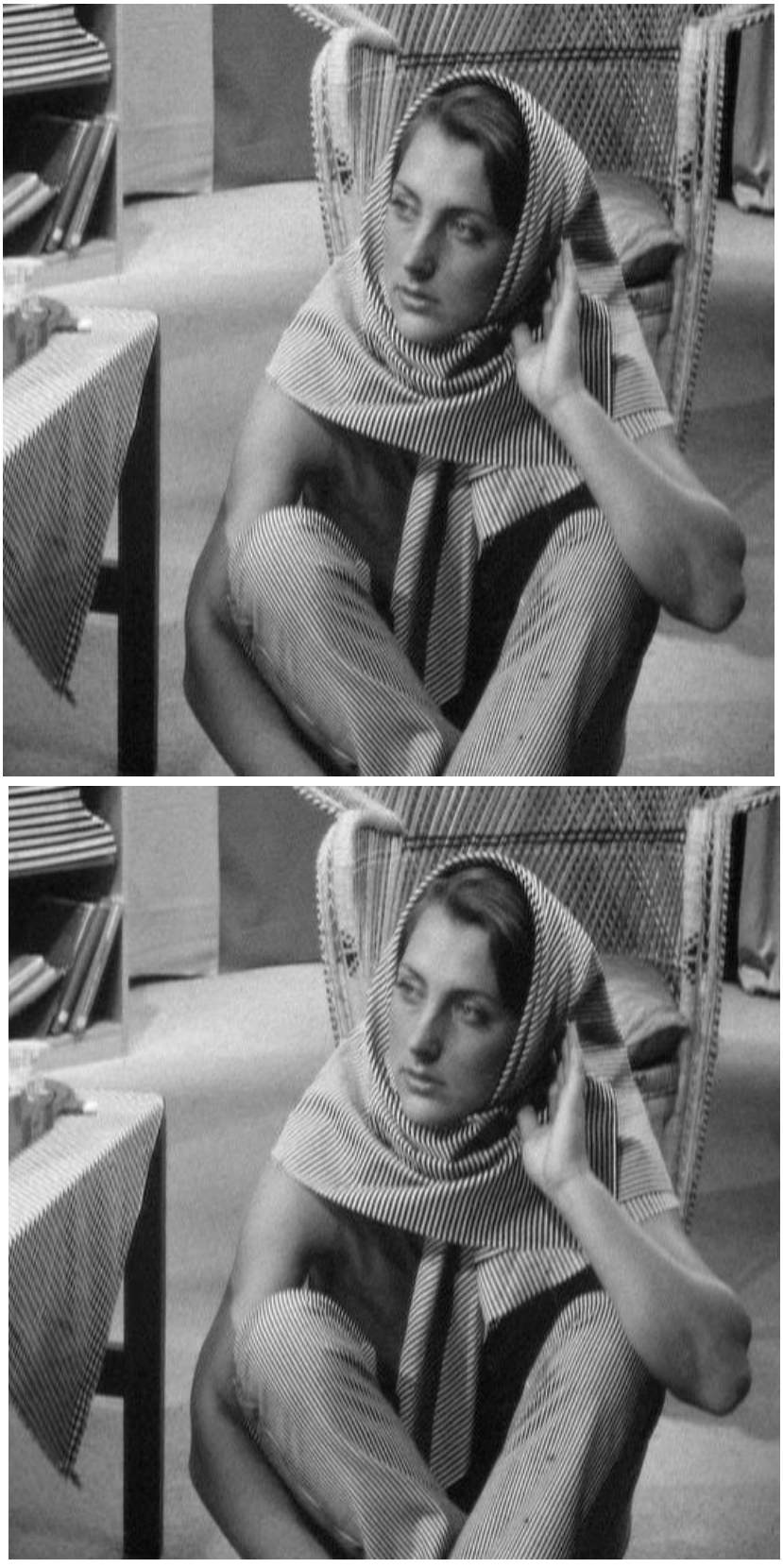

Figure 14: Top: f. Bottom: $u + v$ with $\lambda = 0.2$, $\mu = 0.01$, 100 iterations, $p = 1$.

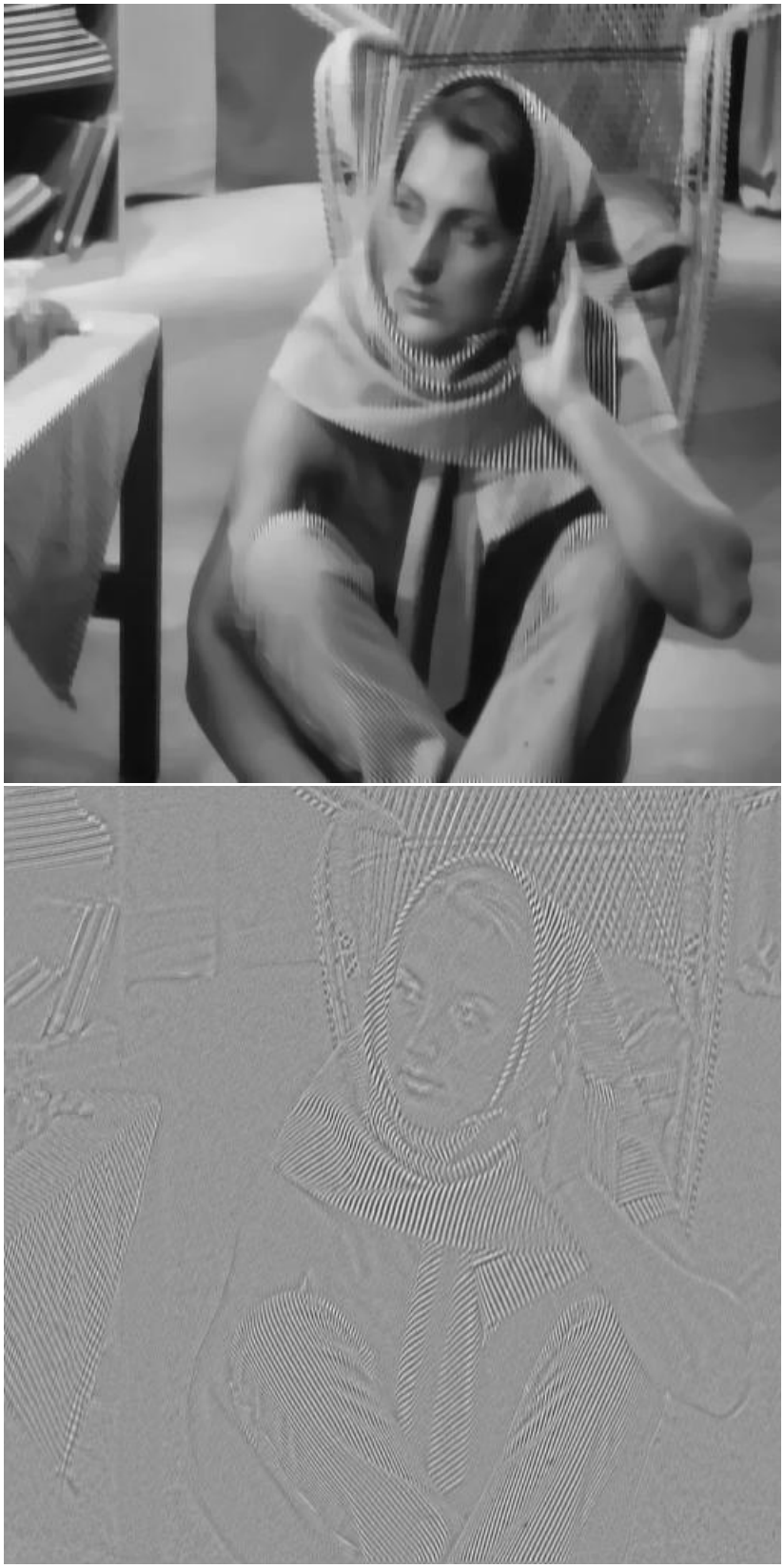

Figure 15: u (top) and v (bottom) components for the image in Fig. 14.

5 Concluding remarks

In this paper, we have shown how we can decompose a given image u_0 into the sum $u + v$, where $u \in BV$ is a function of bounded variation (a cartoon representation of u_0), and v is an oscillatory function, representing random noise or texture. We have also shown how the method can be used to texture segmentation and texture discrimination. The proposed model combines the idea of the total variation minimization in image restoration of Rudin-Osher-Fatemi [22] with the ideas introduced by Y. Meyer [17] for the appropriate space to model texture or noise. At this moment, the model cannot distinguish between noise and texture. We plan to discuss in the future how to denoise the v component, in the case of noisy textured images. Finally, we validate the claims of Yves Meyer on several experimental results, and we show in particular that textures can be defined and represented only using two functions $\vec{g} = (g_1, g_2)$. This is different from the wavelet decomposition techniques or from the use of the Gabor transform.

Acknowledgments

The authors would like to thank Guillermo Sapiro for suggesting some related references, Eitan Tadmor for valuable conversations on this subject, and Richard Tsai, for discussions on the numerical discretization.

References

[1] R. Acart and C.R. Vogel, *Analysis of bounded variation penalty methods of ill-posed problems*, Inverse Problem 10, pp. 1217-1229, 1994.

[2] L. Alvarez, F. Guichard, P.L. Lions, J.-M. MOREL, *Axioms and fundamental equations of image-processing*, Archive for Rational Mechanics and Analysis, 123 (3), pp. 199-257, 1993.

[3] F. Andreu, C. Ballester, V. Caselles, J.M. Mazon, *Minimizing total variation flow*, CRAS I-Mathématique, 331 (11), pp. 867-872, 2000.

[4] F. Andreu, V. Caselles, J.I. Diaz, J.M. Mazon, *Some qualitative properties for the total variation flow*, Journal of Functional Analysis, 188 (2), pp. 516-547, 2002.

[5] G. Aubert and L. Vese, *A variational method in image recovery*, Siam Journal on Numerical Analysis, 34(5), pp. 1948-1979, 1997.

[6] C. Ballester and M. Gonzalez, *Affine invariant texture segmentation and shape from texture by variational methods*, J. Math. Imaging Vis. 9 (2), pp. 141-171, 1998.

[7] S. Casadei, S. Mitter, and P. Perona, *Boundary detection in piecewise homogeneous textured images*, Lecture Notes in Computer Science, Vol. 588, pp. 174-183, 1992.

[8] T. Chan and L. Vese, *An active contour model without edges*, in "Scale-Space Theories in Computer Vision", Lecture Notes in Computer Science Vol. 1682 , pp. 141-151, 1999.

[9] T.F. Chan and L.A. Vese, *Active contours without edges*, IEEE Transactions on Image Processing, Vol. 10(2), pp. 266 -277, 2001.

[10] A. Chambolle and P.L. Lions, *Image recovery via total variation minimization and related problems*, Numer. Math. 76, pp. 167-188, 1997.

[11] L.C. Evans and R.F. Gariepy, *Measure Theory and Fine Properties of Functions*, CRC Press, London 1992.

[12] G. Koepfler, C. Lopez and J.-M. Morel, *A multiscale algorithm for image segmentation by variational method*, SIAM J. Num. Analysis, 31(1), pp. 282-299, 1994.

[13] T.S. Lee, *A Bayesian framework for understanding texture segmentation in the primary visual-cortex*, Vision Research, 35 (18), pp. 2643-2657, 1995.

[14] T.S. Lee, D. Mumford, and A. Yuille, *Texture segmentation by minimizing vector-valued energy functionals - the coupled-membrane model*, Lecture Notes in Computer Science, Vol. 588, pp. 165-173, 1992.

[15] F. Malgouyres, *Mathematical analysis of a model which combines total variation and wavelet for image restoration*, Technical Report of Université Paris 13.

[16] F. Malgouyres, *Minimizing the total variation under a wavelet style constraint for image restoration*, UCLA CAM Report 01-23.

[17] Y. Meyer, *Oscillating Patterns in Image Processing and Nonlinear Evolution Equations*, University Lecture Series Volume 22, AMS 2002.

[18] D. Mumford and J. Shah, *Optimal approximations by piecewise smooth functions and associated variational-problems*, Communications on Pure and Applied Mathematics, 42 (5), pp. 577-685, 1989.

[19] F. Oru, *Le rôle des oscillations dans quelques problèmes d'analyse non-linéaire*, Thèse, CMLA, ENS-Cachan, June 9, 1998.

[20] P. Perona and J. Malik, *Scale-space and edge-detection using anisotropic diffusion*, IEEE on PAMI, 12 (7), pp. 629-639, 1990.

[21] L. Rudin and S. Osher, *Total variation based image restoration with free local constraints*, Proc. IEEE ICIP, Vol. I, pp. 31-35, Austin (Texas) USA, 1994.

[22] L. Rudin, S. Osher and E. Fatemi, *Nonlinear total variation based noise removal algorithms*, Physica D, 60, pp. 259-268, 1992.

[23] B. Sandberg, T. Chan and L. Vese, *A Level-Set and Gabor-Based Active Contour Algorithm for Segmenting Textured Images*, UCLA CAM Report 02-39, 2002.

[24] G. Sapiro, *Color Snakes*, Computer Vision and Image Understanding, 68 (2), pp. 247-253, 1997.

[25] L. Vese, *A study in the BV space of a denoising-deblurring variational problem*, Applied Mathematics and Optimization, 44 (2), pp. 131-161, 2001.

[26] W.M. Wells, III, W.E.L. Grimson, R. Kikinis, and F.A. Jolesz, *Adaptive Segmentation of MRI Data*, IEEE Transactions on Medical Imaging, Vol. 15, No. 4, 1996.

[27] S.C. Zhu, Y.N. Wu, and D. Mumford, *Filters, random fields and maximum entropy (FRAME): Towards a unified theory for texture modeling*, International Journal of Computer Vision, 27(2), pp. 107-126, 1998.

[28] S.C. Zhu, Y.N. Wu, and D. Mumford, *Minimax entropy principle and its application to texture modeling*, Neural Computation, 9 (8), pp. 1627-1660, 1997.